Improving animal-specific radiotherapy quality assurance for kilovoltage X-ray radiotherapy using a 3D printed dog skull water phantom

Yoshinori Tanabe[1]* 🆔, Toshie Iseri[2] 🆔, Ryouta Onizuka[3] 🆔, Takayuki Ishida[4] 🆔, Hidetoshi Eto[5] 🆔
and Munekazu Nakaichi[6] 🆔

[1]*Faculty of Medicine, Graduate School of Health Sciences, Okayama University, Okayama, Japan*
[2]*Faculty of Agriculture, Animal Medical Emergency Center, Tokyo University of Agriculture and Technology, Fuchu, Japan*
[3]*Department of Radiology, Kokura Memorial Hospital, Kitakyusyu, Japan*
[4]*Division of Health Sciences, Graduate School of Medicine, Osaka, Japan*
[5]*Department of Radiology, Yamaguchi University Hospital, Ube, Japan*
[6]*Joint Faculty of Veterinary Medicine, Yamaguchi University, Yamaguchi, Japan*

Abstract

Background: Accurate dose assessment during animal radiotherapy is beneficial for veterinary medicine and medical education.

Aim: To visualize the radiation treatment distribution of orthovoltage X-ray equipment in clinical practice using Monte Carlo simulations and create a dog skull water phantom for animal-specific radiotherapy.

Methods: EGSnrc-based BEAMnrc and DOSXYZnrc codes were used to simulate orthovoltage dose distributions. At 10, 20, 30, 40, 50, and 80 mm in a water phantom, the depth dose was measured with waterproof Farmer dosimetry chambers, and the diagonal off-axis ratio was measured with Gafchromic EBT3 film to simulate orthovoltage dose distributions. Energy differences between orthovoltage and linear accelerated radiotherapy were assessed with a heterogeneous bone and tissue virtual phantom. The animal-specific phantom for radiotherapy quality assurance (QA) was created from CT scans of a dog and printed with a three-dimensional printer using polyamide 12 nylon, with insertion points for dosimetry chambers and Gafchromic EBT3 film.

Results: Monte Carlo simulated and measured dose distributions differed by no more than 2.0% along the central axis up to a depth of 80 mm. The anode heel effect occurred in shallow areas. The orthovoltage radiotherapy percentage depth dose in bone was >40%. Build-up was >40%, with build-down after bone exit, whereas linear accelerator radiotherapy absorption changed little in the bone. A highly water-impermeable, animal-specific dog skull water phantom could be created to evaluate dose distribution.

Conclusion: Animal-specific water phantoms and Monte Carlo simulated pre-treatment radiotherapy are useful QA for orthovoltage radiotherapy and yield a visually familiar phantom that will be useful for veterinary medical education.

Keywords: Orthovoltage, Animal radiotherapy, Heel effect, Water animal phantom, Animal specific radiotherapy quality assurance.

Introduction

Small animal radiotherapy requires high treatment accuracy and animal-specific radiotherapy quality assurance (QA) (Iseri *et al.*, 2022). Dose accuracy in animal models has been studied as a way to estimate the radiation response of tumors and normal tissues (Verhaegen *et al.*, 2018).

Kilovoltage X-rays delivered via orthovoltage equipment (Philips Medical Systems, Best, The Netherlands) for small animal radiotherapy are widely used in facilities ranging from clinics to university hospitals (Pampena *et al.*, 2016; Seo *et al.*, 2018). The use of linear accelerators for animal radiotherapy has increased in some facilities but remains rare due to high costs and large machine sizes (Seo *et al.*, 2018). The absorbed dose during orthovoltage radiotherapy may be measured using water procedures (Ma *et al.*, 2001) to ensure that the prescribed doses for soft tissue are accurate. However, differences in tissue density throughout the body (e.g., lung and bone) make it difficult to predict dose distribution in clinical use accurately. Equipment and patient-specific QA are important for identifying discrepancies between calculated and delivered radiation doses and assessing algorithm-based management of heterogeneities and other factors (Miften *et al.*, 2018; Tanabe *et al.*,

2020). Orthovoltage radiotherapy is delivered in high prescription doses, similar to linear accelerator radiotherapy (Medina *et al.*, 2008; Pampena *et al.*, 2016), but manufacturers generally do not sell radiation treatment planning systems.

Monte Carlo simulation is an established method for estimating radiation treatment dose (Andreo, 1991; Onizuka *et al.*, 2018; Iseri *et al.*, 2023), including for orthovoltage radiotherapy dose distribution (Abbas *et al.*, 2014). If the orthovoltage dose distribution can be understood, this technique may be an effective tool for selecting either orthovoltage or linear accelerator radiotherapy when considering dosing around radiosensitive organs. Ye, there is little time to teach about radiation therapy in veterinary education. Using visual simulation images and animal-specific verification devices can aid in our understanding of the physical events of radiation in a short time (Azer and Azer, 2016).

Three-dimensional (3D) printers are widely used in radiotherapy research to create phantoms from processed CT images (Ji *et al.*, 2017; Kamomae *et al.*, 2017). The accuracy of 3D printers depends on the printing materials and image processing methods. The accuracy required for QA verification is within 1 mm (Miften *et al.*, 2018), and engineering technology and knowledge are essential for creating high-quality phantoms.

To the best of our knowledge, there are no prior reports on using a 3D-printed dog skull water phantom for pre-treatment QA of orthovoltage radiotherapy dose. Therefore, we investigated the ability of Monte Carlo simulations and physical phantom measurements to predict dose distributions with conventional orthovoltage X-ray equipment and enable the creation of a dog skull water phantom that could be used for QA. Additionally, the suitability of orthovoltage radiotherapy was compared with accelerated linear radiotherapy.

Materials and Methods

This study used a self-contained industrial orthovoltage X-ray system (output voltage range 32–320 kV, tube current range 3–30 mA; Philips Medical Systems, Best, The Netherlands) generally used for small animal radiotherapy. The unit has several applicator cones, a field size of $\varphi 4.0$ cm, and a treatment distance of 50 cm.

Monte Carlo simulation for orthovoltage radiotherapy

Monte Carlo orthovoltage dose distributions were simulated with EGSnrc-based BEAMnrc and DOSXYZnrc codes using MATLAB from the NRCC group (Kawrakow, 2000; Kawrakow *et al.*, 2011). The orthovoltage apparatus consists of a target, X-ray tube window, primary collimator, and mirror. The geometric dimensions and materials of each component module were provided by vendors and obtained from reference tables (Knöös *et al.*, 2007; Abbas *et al.*, 2014). The incident electron energy was set to 300 kV, with an added filtration of 2.0 mm aluminum and 0.5 mm copper. The percentage dose depth was measured at 10, 20, 30, 40, 50, and 80 mm with standard PTW 30013 0.6 cc waterproof Farmer ionization chambers (PTW, Freiburg, Germany) in a WP1D water phantom (IBA Dosimetry, Schwarzenbruck, Germany), and these physical measurements in the water phantom were used as comparators for the simulated doses. The diagonal off-axis ratio for each depth was measured with the Gafchromic EBT3 film (Ashland Advanced Materials, Bridgewater, NJ) and a tough water phantom (Kyoto Kagaku, Kyoto, Japan) to model the distribution spread for the Monte Carlo simulation.

Evaluation of dose distribution between kV energy and MV energy

The dose distributions in the model dog CT image were compared to those in the Monte Carlo simulations for this study's orthovoltage radiotherapy and those for an Agility MV voltage linear accelerator (Elekta AB, Stockholm, Sweden) using previously published models (Onizuka *et al.*, 2018).

In the Monte Carlo simulation, we assessed the effects of energy differences on bone by creating a heterogeneous bone and tissue phantom consisting of a 1.0 cm thick layer of water above a 1.0 cm wide layer of cortical bone (physical density $\rho = 1.40$ g/cm³) and a 10 cm layer of water. Dose profiles were compared between orthovoltage radiotherapy (energy 300 KeV and a field size of 4.0×4.0 cm²) and the Agility MV voltage linear accelerator (6 MV and a field size of 4.0×4.0 cm²).

Printing of the dog skull water phantom

The 3D-printed dog, skull water phantom, was modeled on a medium-sized Shiba Inu (~12 kg) suitable for treatment with orthovoltage or linear accelerator radiotherapy. First, using a 3D workstation (Ziostation-2; Ziosoft/AMIN, Tokyo, Japan), 3D CT raw images of the dog were processed for erosion. Structures other than the 3 mm surface were removed from the picture after subtraction processing, and an STL image of only the 3 mm thick surface was created. Next, using the CAD STL data editing software GeoMagic Design X (3D Systems, Rock Hill, SC) and SOLIDWORKS 3D CAD Premium 2020 (Dassault Systèmes, Vélizy-Villacoublay, France), a dog-shaped water phantom was designed that included insertion points for the Farmer chamber dosimeters and two Gafchromic films. A RaFaEl II plus 300C-HT 3E printer (Aspect Co., Tokyo, Japan) was used to create the phantom with polyamide 12 nylon (Rahim *et al.*, 2016) to make it impermeable to water, and an acrylic paint was applied to the surface to suppress gas permeability (Table 1).

Results

Figure 1 shows the radiation dose profile along the axis, measured at 5, 10, 15, 20, 30, 40, 50 and 80 mm depths. Table 2 shows the dose ratio difference up to 10 mm off-axis on each side (the anode heel effect). The in-plane

Table 1. Material and geometry information for a dog skull water phantom.

Dog skull water phantom	
3D printing	Additive manufacturing techniques
Material	Polyamide 12 nylon
Specific gravity	1.03
Particle size (μm)	45 ± 5
Joining	Cemedine PPX
Surface coating	Acrylic paint
Distance from the center of the farmer chamber to the surface (mm)	16.0
Distance from Gafchromic film (1st) to surface (mm)	33.2
Distance from Gafchromic film (1st) to nose surface (mm)	15.0
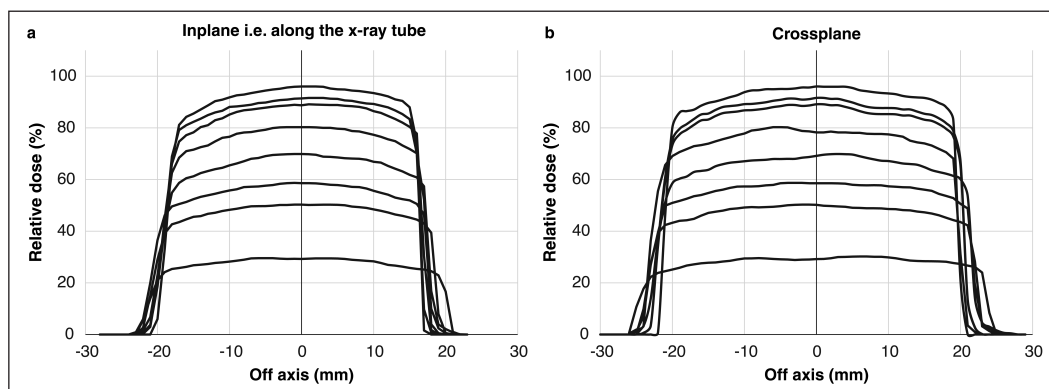
Fig. 1. Measured dose profiles along the two axes using film (a: in plane i.e., along the X-ray tube; b: cross plane). This figure was referred the Figure 3 of reference Iseri *et al.*, 2023.

dose along the profile was reduced by 1% to 15 mm on the anode side. The irradiation diameter obtained at a dose of 50% at a depth of 2 cm was asymmetric (in plane 3.64 cm; cross plane 4.26 cm).

Figure 2 shows the Monte Carlo simulation percentage depth dose and the measured percentage depth dose. The dose difference between the measured dose and beam modeling was adjusted to within at least 2.0% along the central axis.

Figure 3 shows the radiation dose distributions estimated by Monte Carlo simulations for linear accelerator radiotherapy under near-irradiation conditions and for orthovoltage radiation. The absorbed dose to the skull near the surface with orthovoltage radiation was similar to that of the single port irradiation, and the reduction rate of orthovoltage radiation was high.

The percentage depth dose in bone with orthovoltage radiotherapy was more than 40%. With orthovoltage radiotherapy, a build-up of more than 40% was seen in the bone region, with build-down after bone transmission (Fig. 4a). With linear accelerator radiotherapy, there was little change in absorption in the bone region, although a slight rebound was seen after bone transmission (Fig. 4b).

Figure 5 shows the water phantom that was created using a 3D printer. The dog skull water phantom was water impermeable, had inserts for Farmer dosimetry chambers and two sheets of Gafchromic film, and could be used to perform animal-specific radiotherapy QA.

Discussion

In small animals, radiotherapy is often performed in shallow areas. The use of Monte Carlo simulations to aid dosimetry is helpful for evaluating dose distribution, but in veterinary medicine education, visual simulation phantoms can be quicker to use and learn from. In this study, the use of simulated doses and measurements in a water phantom provided us with an understanding that could be applied to create a 3D printed animal-specific dog skull water phantom with appropriate inserts for dosimetry chambers and Gafchromic sheets that was water impermeable and had high gas impermeability and permitted pre-treatment radiotherapy QA.

As shown by the results of the off-axis ratios, the heel effect is seen at a shallow depth of about 1.5 cm, a finding that is reflected in past research (Knöös *et al.*, 2007; Azim *et al.*, 2015). The radiation field size was asymmetric, which may change over time because this

Table 2. The ratio of dose difference for10 mm off axis at each side.

| Depth (mm)	5	10	15	20	30	40	50	80
In plane (%)	−1.78	−1.26	−1.49	−0.96	−0.55	0.22	−0.32	−0.33
Cross plane (%)	0.51	0.74	0.74	0.4s2	−0.11	−0.10	0.00	−0.21
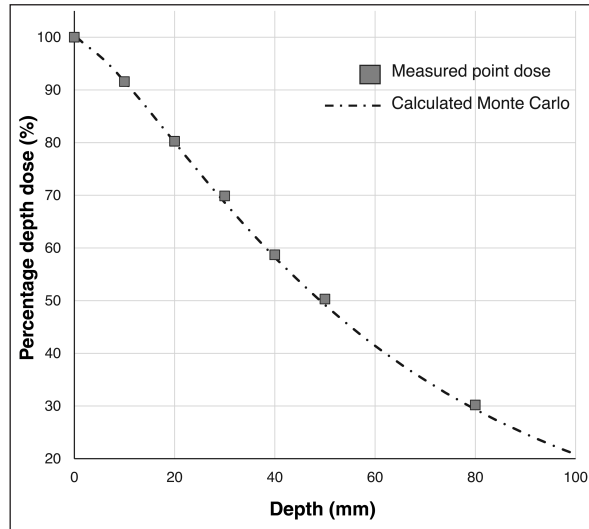
Fig. 2. Depth dose curves for orthovoltage radiotherapy. The graph compares a Monte Carlo simulation and water measurements. This figure was referred the Figure 2 of reference Iseri *et al.*, 2023.
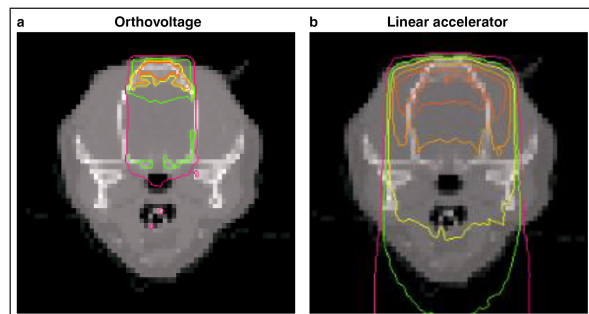
Fig. 3. Dose distribution using Monte Carlo simulations (a: orthovoltage radiotherapy; b: linear accelerator radiotherapy).

study's orthovoltage machine was made more than 20 years after its introduction. Additionally, since vendors fine-tune the beam quality and target angle at each facility, we believe that beam modeling per facility, as for linear accelerator equipment, is essential.

Based on the comparison of orthovoltage and linear accelerator radiotherapy, the absorbed dose was similar to that of the linear accelerator in the bone near the surface. Still, the orthovoltage radiation had more excellent attenuation as bone depth increased. The interaction between photons and matter is greatly affected by the energy range. The photoelectric effect region for orthovoltage radiation is affected by atomic
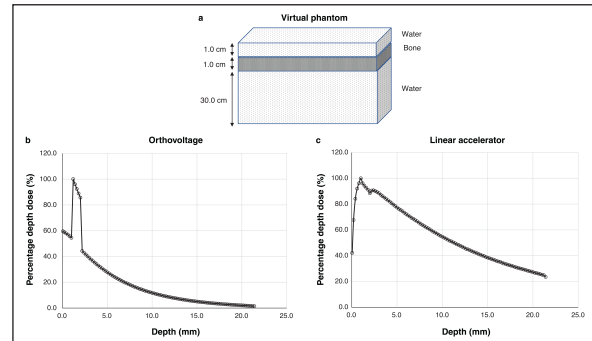

Fig. 4. Dose curve for the heterogeneous bone and tissue phantom (a: virtual phantom setting; b: the dose curve with orthovoltage radiotherapy; c: the dose curve of the linear accelerator radiotherapy).

number, in contrast to the Compton scattering region, which affects linear accelerator radiation (Jones *et al.*, 2018). We believe that visualizing the dose distribution accuracy of orthovoltage radiotherapy for veterinary medicine is helpful in evaluating targets and at-risk organs. Furthermore, the dose distribution serves as a criterion for selecting either orthovoltage or linear accelerator radiotherapy. In addition, the dose measurement for the surface as a crystalline lens generally uses a Gafchromic film and solid water phantom. However, this study method could be measured in near clinical conditions by placing a Gafchromic film on the eyes of the dog phantom, and the dose of the crystalline lens could be evaluated using Monte Carlo simulations.

The major limitation of this study is that since the measurement position of the animal phantom is fixed, its degrees of freedom are lower than those of a solid water phantom. It is, therefore, necessary to understand the merits of both. However, education on radiation therapy in veterinary medicine is limited. The water dog phantom makes it possible to understand the differences in dose between the orthovoltage and linear accelerator radiotherapy with a familiarly shaped animal phantom rather than a rectangular phantom. Therefore we believe we can help improve and reduce the time needed for radiotherapy veterinary education with our method for creating animal-specific phantoms. In this study, a 3D printer was able to create an accurate water impermeable phantom using the knowledge and technical cooperation of the engineering department. Dose evaluation can be performed using medical experience and knowledge, illustrating that cooperation between veterinary medicine, medicine, and engineering is effective.
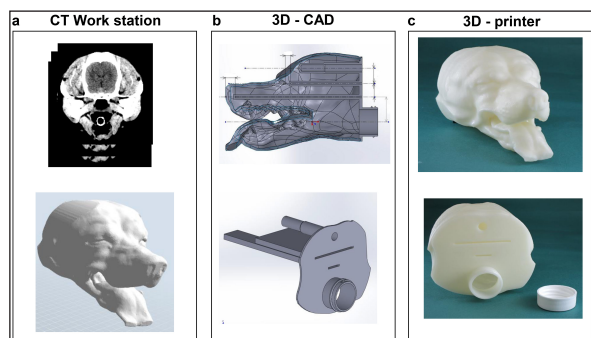
Fig. 5. Workflow for creating the dog skull water phantom (a: 3D workstation; b: 3D-CAD; c: 3D printer).

Conclusion

By using Monte Carlo simulations, physical phantom measurements, and a 3D printer, we could visualize the radiation treatment distribution of orthovoltage X-ray equipment in clinical practice. This technique will be beneficial for animal-specific radiotherapy QA and veterinary medicine education.

Conflict of interest

The authors declare no conflicts of interest.

Authors' contributions

YT, IT, RO, and MN were involved in study design and data interpretation. IT and HE were involved in data analysis. All authors critically revised the report, commented on the drafts of the manuscript, and approved the final word.

References

Abbas, H., Mahato, D.N., Satti, J. and MacDonald, C.A. 2014. Measurements and simulations of focused beam for orthovoltage therapy. Med. Phys. 41, 041702.

Andreo, P. 1991. Monte Carlo techniques in medical radiation physics. Phys. Med. Biol. 36, 861–920.

Azer, S.A. and Azer, S. 2016. 3D anatomy models and impact on learning: a review of the quality of the literature. Health. Prof. Educ. 2, 80–98.

Azim, R., Alaei, P., Spezi, E. and Hui, S.K. 2015. Characterization of an orthovoltage biological irradiator used for radiobiological research. J. Radiat. Res. 56, 485–492.

Iseri, T., Tanabe, Y., Horikirizono, H., Sunahara, H., Itoh, H., Nemoto, Y., Itamoto, I., Tani, K., Tanaka, H. and Nakaichi, M. 2022. Adjustment of multi-leaf collimator parameters in 4-MV and 6-MV IMRT: a study of veterinary clinical cases. Open. Vet. J. 12, 407–413.

Iseri, T., Tanabe, Y., Onizuka, R., Torigoe, Y., Horikirizono, H., Itamoto, K., Sunahara, H., Itoh, H., Tani, K. and Nakaichi, M. 2023. A Monte Carlo study on dose distribution of an orthovoltage radiation therapy system. Phys. Eng. Sci. Med; https://doi.org/10.1007/s13246-023-01237-4.

Ji, Z., Jiang, Y., Guo, F., Sun, H., Fan, J., Zhang, L. and Wang, J. 2017. Dosimetry verification of radioactive seed implantation for malignant tumors assisted by 3D printing individual templates and CT guidance. Appl. Radiat. Isot. 124, 68–74.

Jones, K.C., Redler, G., Templeton, A., Bernard, D., Turian, J. and Chu, J.C.H. 2018. Characterization of compton-mptonnd imaging with an analytical simulation method. Phys. Med. Biol. 63, 025016.

Kamomae, T., Shimizu, H., Nakaya, T., Okudaira, K., Aoyama, T., Oguchi, H., Komori, M., Kawamura, M., Ohtakara, K., Monzen, H., Itoh, Y. and Naganawa, S. 2017. Three-dimensional printer-generated patient-specific phantom for artificial *in vivo* dosimetry in radiotherapy quality assurance. Phys. Med. 44, 205–211.

Kawrakow, I. 2000. Accurate condensed history Monte Carlo simulation of electron transport. I. EGSnrc, the new EGS4 version. Med. Phys. 27, 485–498.

Kawrakow, I., Mainegra-Hing, E., Rogers, D.W.O., Tessier, F. and Walters, B.R.B. 2011. The EGSnrc code system: Monte Carlo simulation of electron and photon transport. National Research Council of Canada Report PIRS, p: 701.

Knöös, T., Rosenschöld, P.M. and Wieslander, E. 2007. Modelling of an orthovoltage X-rthovoltage oltage ovoltagEGSnrc Monte Carlo package. J. Phys. Conf. Ser. 74, 021009.

Ma, C.M., Coffey, C.W., DeWerd, L.A., Liu, C., Nath, R., Seltzer, S.M. and Seuntjens, J.P. 2001. AAPM protocol for 40-300 kV X-ray beam dosimetry in radiotherapy and radiobiology. Med. Phys. 28, 868–893.

Medina, L.A., Herrera-Penilla, B.I., Castro-Morales, M.A., García-López, P., Jurado, R., Pérez-Cárdenas, E., Chanona-Vilchis, J. and Brandan, M.E. 2008. Use of an orthovoltage X-ray treatment unit as a radiation research system in a small animal cancer model. J. Exp. Clin. Cancer. Res. 27, 57.

Miften, M., Olch, A., Mihailidis, D., Moran, J., Pawlicki, T., Molineu, A., Li, H., Wijesooriya, K., Shi, J., Xia, P., Papanikolaou, N. and Low, D.A. 2018. Tolerance limits and methodologies for IMRT measurement-based verification QA: recommendations of AAPM task group no. 218. Med. Phys. 45, e53–e83.

Onizuka, R., Araki, F. and Ohno, T. 2018. Monte Carlo dose verification of VMAT treatment plans using elekta agility 160-leaf MLC. Physica. Med. 51, 22–31.

Pampena, R., Palmieri, T., Kyrgidis, A., Ramundo, D., Iotti, C., Lallas, A., Moscarella, M., Borsari, S., Argenziano, G. and Longo, C. 2016.

Orthovoltage radiotherapy for nonmelanoma skin cancer (NMSC): comparison between 2 different schedules. J. Am. Acad. Dermatol. 74, 341–347.

Rahim, T.N.A.T., Abdullah, A.M., Akil, H.M. and Mohamad, D. Comparison of mechanical properties for polyamide 12 composite-based biomaterials fabricated by fused filament fabrication and injection molding. In AIP Conference Proceedings, 2016, p 1791.

Seo, J., Son, J., Cho, Y., Park, N., Kim, D.W., Kim, J. and Yoon, M. 2018. Kilovoltage radiotherapy for companion animals: dosimetric comparison of 300 kV, 450 kV, and 6 MV X-ray beams. J. Vet. Sci. 9, 550–556.

Tanabe, Y., Ishida, T., Eto, H., Sera, T., Emoto, Y. and Shimokawa, M. 2020. Patient-specific radiotherapy quality assurance for estimating actual treatment dose. Med. Dosim. 46, e5–e10.

Verhaegen, F., Dubois, L., Gianolini, S., Hill, M.A., Karger, C.P., Lauber, K., Kevin M.P., David, S., Thorwarth, D., Vanhove C., Vojnovic, B., Weersink, R., Wilkensl, J.J. and Georg, D. 2018. ESTRO ACROP: technology for precision small animal radiotherapy research: optimal use and challenges. Radiother. Oncol. 126, 471–478.